



Milankovitch Theory “as an Initial Value Problem”

Mikhail Y. Verbitsky^{1,2}

¹Gen5 Group, LLC, Newton, MA, USA

²UCLouvain, Earth and Life Institute, Louvain-la-Neuve, Belgium

Correspondence: Mikhail Verbitsky (verbitskys@gmail.com)

Abstract.

The dynamics of large ice sheets is fundamentally defined by the advection of mass and temperature. The timescale of these processes is critically dependent on the surface mass balance. Because of the ice-climate system's nonlinearity, its response to the orbital forcing in terms of engagement of negative and positive feedbacks is not symmetrical. This asymmetry may reduce the effective mass influx, and the resultant advection timescale may become longer, which is equivalent to the increased system's memory of its initial conditions. In this case the Milankovitch theory becomes an initial value problem: Depending on initial conditions, for the same orbital forcing and for the same balance between terrestrial positive and negative feedbacks, the historical glacial rhythmicity could have been dominated either by the eccentricity period of ~100 kyr, or by the doubled obliquity period of ~80 kyr, or by a combination of both.

1. Introduction.

Though modelling of the late Pleistocene ice-age history using space resolving three-dimensional models (e.g., Abe-Ouchi *et al*, 2013) and models of intermediate complexity (e.g., Ganopolski and Calov, 2011) are now computationally affordable and may be insightful, the dynamical paleoclimatology (the term was coined by Barry Saltzman, 2002) remains to be a powerful and may be even a preferable tool to study climate evolution on orbital timescales. Even if we put aside the esthetical attractiveness of dynamical models (in the sense of Paul Dirac's vision that a physical law must indeed possess mathematical beauty), there are important physical considerations that make them essential. The first fundamental concern, that even three-dimensional models are not able to comprehensively address, relates to the fact that the ice-sheet volume is controlled by a small difference of two big values, accumulation and ablation, and therefore “...in their current state, ice sheet models do not have the predictive power to precisely reconstruct ice sheet history” (Gowan, 2023). The second consideration has been rigorously substantiated by Bahr *et al* (2015) in their review and comparison of glaciers' and ice sheets' scaling solutions versus corresponding three-dimensional models: “...if any of the numerical models' parameters are unknown or have a distribution of possible values... there is no a priori reason to expect that a tuned model will be more accurate than a tuned scaling solution”. This observation is particularly true when the goal of the mathematical modelling is not a regional climate but a history of global ice volume. For these reasons, in our previous work, we derived a dynamical model of glacial rhythmicity based on scaled mass-, momentum-, and heat-conservation equations of non-Newtonian ice flow combined with the energy-balance model of global climate (Verbitsky *et al*, 2018, VCV18 thereafter) and demonstrated that its dynamical properties can be largely defined by only two similarity parameters: (a) the ratio of the orbital forcing amplitude to the amplitude of the terrestrial mass influx, and (b) the so called *V*-number that is the ratio of terrestrial positive-to-negative feedbacks amplitudes (Verbitsky and Crucifix, 2020). Specifically, when the ratio of the orbital forcing amplitude to the amplitude of the terrestrial mass influx is about 1.5 – 2., and the positive feedbacks in the system are well articulated, i.e., $V \sim 0.7 - 1.$, the system produces the obliquity-period doubling bifurcation.



47 Although the astronomical forcing is the result of the celestial mechanics, and the orbital periods such
48 as the precession, obliquity, and eccentricity periods are used to be accepted almost like physical
49 constants, the amplitude of this forcing, as a component of the global ice mass balance, is defined much
50 less precisely. It would be of a considerable interest therefore to study a dynamical system behavior when
51 the ratio of the orbital forcing amplitude to the amplitude of the terrestrial mass influx is somewhat less
52 than 1.5.

53 The VCV18 model is based on the thin-viscous-boundary-layer approximation of ice flow. Therefore,
54 its dynamics is largely defined by the advection of mass and temperature. The timescale of these
55 processes is critically dependent on the surface mass balance, i.e., accumulation minus ablation. When the
56 orbital forcing, that is an important player of the surface mass balance, is neither strong enough to engage
57 sufficient positive feedbacks, nor small enough to be overwhelmed by the terrestrial mass influx, the
58 resultant effective mass influx affected by negative feedbacks may become smaller, the advection
59 timescale may become longer and this is equivalent to the increased system's memory of its initial
60 conditions. Thus the theory of Pleistocene glacial rhythmicity, i.e., the Milankovitch theory, becomes an
61 initial value problem. Though the title of our paper obviously alludes to Saltzman's (1962) landmark
62 work, we do not necessarily anticipate discovering the deterministic chaos in the VCV18 system. We will
63 demonstrate though that, depending on initial conditions, for the same orbital forcing and for the same
64 balance between terrestrial positive and negative feedbacks, the Pleistocene glacial rhythmicity could
65 have been dominated either by the eccentricity period of ~100 kyr, or by the doubled obliquity period of
66 ~80 kyr, or by a combination of both.

68 2. The experiments

69
70 The model we utilize here has been described and analyzed in the series of publications, i.e., VCV18,
71 Verbitsky and Crucifix (2020, 2023), and Verbitsky (2022):

$$73 \frac{dS}{dt} = \frac{4}{5} \zeta^{-1} S^{3/4} (\hat{a} - \varepsilon F - \kappa \omega - c\theta) \quad (1)$$

$$74 \frac{d\theta}{dt} = \zeta^{-1} S^{-1/4} (\hat{a} - \varepsilon F - \kappa \omega) \{ \alpha \omega + \beta [S - S_0] - \theta \} \quad (2)$$

$$75 \frac{d\omega}{dt} = -\gamma [S - S_0] - \frac{\omega}{\tau} \quad (3)$$

76
77 Here, S (m²) is the area of an ice sheet, θ (°C) is the ice-sheet basal temperature, and ω (°C) is the global
78 "rest-of-the-climate" temperature. Equation (1) is the ice mass balance $\frac{d(HS)}{dt} = AS$, where the ice
79 thickness H is determined from the thin-viscous-boundary-layer approximation of ice flow, $H = \zeta S^{1/4}$, ζ
80 is dimensional factor (Verbitsky, 1992) and $A = \hat{a} - \varepsilon F - \kappa \omega - c\theta$ is the surface mass influx. Equation
81 (2) describes vertical ice-temperature advection, and equation (3) is the climate energy-balance equation.
82 More specifically, \hat{a} (m s⁻¹) is the snow precipitation rate; F is adimensional external forcing of the
83 amplitude ε (m s⁻¹); $\kappa \omega$ is "fast" positive feedback of the global climate in ice mass balance; $c\theta$ represents
84 ice-sheet basal sliding combining positive feedback, $\alpha \omega$, and a negative feedback $\beta [S - S_0]$ (both are
85 "slow" due to the vertical temperature advection). The term $-\gamma [S - S_0]$ is albedo forcing for global
86 temperature. Remaining parameters κ (m s⁻¹ °C⁻¹), c (m s⁻¹ °C⁻¹), α (adimensional), β (°C m⁻²) and γ (°C m⁻²
87 s⁻¹) are sensitivity coefficients; S_0 (m²) is a reference glaciation area; and τ (s) is the global-temperature
88 timescale.

89 For the purpose of this study, all model parameters are fixed at their reference VCV18 values, such
90 that in all experiments $V = 0.75$, i.e. the terrestrial positive feedbacks are well articulated relative to the
91 negative feedbacks. The only values that are going to be changed will be the initial area of an ice sheet
92 $S(0)$ (10⁶ km²) and the adimensional amplitude of the astronomical forcing that, instead of the mid-June
93 insolation at 65° latitude, used in VCV18, will be modeled as the following:

94



95
$$F = \varepsilon_p \left(\sin \left(\frac{2\pi t}{19} \right) + \sin \left(\frac{2\pi t}{23} \right) \right) + \varepsilon_o \sin \left(\frac{2\pi t}{41} \right) \quad (4)$$

96

97 Here t (kyr) is time, and ε_p and ε_o are adimensional amplitudes of the precession and obliquity
 98 correspondingly. The first two terms replicate eccentricity-modulated precession, and the last term
 99 represents the obliquity forcing. We will now describe five numerical experiments.

100

101 **2.1 Pure eccentricity-modulated precession, $F = 1 \cdot \left(\sin \left(\frac{2\pi t}{19} \right) + \sin \left(\frac{2\pi t}{23} \right) \right)$.**

102

103 The results of the first experiment are presented in Figure 1. As it could be expected (e.g., Abe-Ouchi
 104 *et al*, 2013, Ganopolski, 2024), without obliquity, the system response is dominated by the eccentricity
 105 period (110 kyr in our case). Most importantly, though the time series are obviously not identical for
 106 different initial conditions, the dominant period of the system response is independent of initial
 107 conditions. This independence is preserved also for other values of the precession amplitude, $\varepsilon_p < 1$
 108 (these results are not being presented in Figure 1). The memory of the system about its initial conditions
 109 does not exceed ~50 kyr.

110

111 **2.2 Pure obliquity forcing, $F = \varepsilon_o \sin \left(\frac{2\pi t}{41} \right)$.**

112

113 The results of the next three experiments are presented in Figures 2 – 4. Consistently with VCV18,
 114 when terrestrial positive feedbacks are well articulated ($V = 0.75$) and the amplitude of the obliquity
 115 forcing is strong enough ($\varepsilon_o = 1$, Figure 2), the system exhibits the obliquity-period doubling bifurcation.
 116 The dominant period of the system response (~80 kyr) is not sensitive to the initial conditions. Also like
 117 in VCV18, when terrestrial positive feedbacks are still strong ($V = 0.75$) but the amplitude of the obliquity
 118 forcing is relatively weak ($\varepsilon_o = 0.5$, Figure 3), the system does not bifurcate. The dominant period of the
 119 system response (~40 kyr) is not sensitive to the initial conditions either. The most interesting behavior of
 120 the system is presented in Figure 4 ($\varepsilon_o = 0.7$). It can be observed that, when the orbital forcing is of
 121 intermediate intensity, the relaxation timescale becomes much longer that is equivalent to the increased
 122 system's memory of its initial conditions. Consequently, the dominant period of fluctuations becomes
 123 **sensitive to the initial conditions** and may be either of the obliquity-period or of the double-obliquity-
 124 period value.

125

126 This intriguing phenomenon needs a physical explanation. Because of the system's nonlinearity, its
 127 response to the orbital forcing in terms of engagement of negative and positive feedbacks is not
 128 symmetrical. In the VCV18 model, this may be observed as a shift of the time-mean glaciation area that is
 129 dependent on the effective mass influx. For example, for the reference values of model parameters and
 130 without astronomical forcing, the equilibrium glaciation area $S = 15 \cdot 10^6 \text{ km}^2$. The obliquity forcing of a
 131 relatively small amplitude ($\varepsilon_o = 0.5$, Figure 3) does not engage sufficient positive feedback (it is delayed
 132 due to vertical temperature advection) and the dominant negative feedbacks shift mean glaciation area to
 133 $S = 13.5 \cdot 10^6 \text{ km}^2$ that in the VCV18 model is equivalent to 50% reduction of mean terrestrial mass influx.
 134 The obliquity forcing of a large amplitude ($\varepsilon_o = 1$, Figure 2) administers strong positive feedbacks and
 135 shifts mean glaciation area to $S = 17.7 \cdot 10^6 \text{ km}^2$ that is equivalent to almost doubled mean terrestrial mass
 136 influx. The obliquity forcing of an intermediate amplitude ($\varepsilon_o = 0.7$, Figure 4) shifts mean glaciation area
 137 to $12.3 \cdot 10^6 \text{ km}^2$ that is equivalent to the significant, ten-fold, reduction of terrestrial mass influx.

138

139 The timescale of the advection processes in the “thin” (relative to its horizontal size) ice sheet can be
 140 estimated as $\tau = \frac{H}{\tilde{A}}$, where H is the characteristic ice thickness and \tilde{A} is the mean terrestrial mass influx.
 141 Since $H \sim S^{1/4}$, the timescale in the described experiments is mostly defined by the effective mass influx,
 and the ten-fold reduction of it means ten-fold longer vertical-advection timescale and, consequently, ten-
 fold longer system's memory of its initial conditions. Without astronomical forcing, the relaxation



142 process in the VCV18 dynamical system takes about 100 kyr. The ten-time extension of it implies that the
143 initial conditions of the ice-climate system may be remembered through the entire late Pleistocene.

144

145 **2.3 Eccentricity-modulated precession and obliquity forcing of intermediate intensity,**

146
$$F = 0.7 \left(\sin\left(\frac{2\pi t}{19}\right) + \sin\left(\frac{2\pi t}{23}\right) \right) + 0.7 \sin\left(\frac{2\pi t}{41}\right).$$

147

148 When the system is forced by a combination of eccentricity-modulated precession and obliquity, both
149 with intermediate values of their amplitudes, $\varepsilon_p = \varepsilon_o = 0.7$, the system response, depending on initial
150 conditions, may be dominated either by the eccentricity period of ~100 kyr, or by the doubled obliquity
151 period of ~80 kyr, or by a combination of both (Figures 5 and 6).

152

153 **3. Discussion and Conclusions.**

154

155 The interpretation of the Milankovitch theory that we present in this study is very simple and it is
156 based on very explicit physics:

157

(1) The dynamics of large ice sheets is defined by the advection of mass and temperature;

158

(2) The timescale of ice advection depends mostly on the surface total mass influx;

159

(3) Because of the ice-climate system's nonlinearity, its response to the orbital forcing in terms of
160 engagement of negative and positive feedbacks is not symmetrical. This may change the effective
161 mass influx and the resultant advection timescale;

162

(4) The orbital forcing of a significant amplitude ($\varepsilon_o = 1$) may reduce the internal ice-sheet
163 advection timescale to the value comparable with the obliquity period, and this will produce the
164 obliquity-period doubling bifurcation;

165

(5) The orbital forcing of less intensive amplitude ($\varepsilon_o = 0.7$) may significantly increase the internal
166 ice-sheet advection timescale. It means that the ice-climate system may remember its initial
167 conditions through the entire late Pleistocene, and for the same orbital forcing and for the same
168 balance between terrestrial positive and negative feedbacks, the historical glacial rhythmicity
169 could have been dominated either by the eccentricity period of ~100 kyr, or by the doubled
170 obliquity period of ~80 kyr, or by a combination of both.

171

172 Since we have only one historical time series, our theory cannot, indeed, be verified based on the
173 empirical data, and, instead, other models may need to be involved in a comprehensive test. Obviously,
174 this may be easier said than done. A hypothetical model that would be appropriate for such testing should
175 be able to explicitly account for all the above physics. Therefore, all phenomenological models, obtained
176 either from the fitting to the empirical data or by emulating the behavior of more comprehensive models,
177 will be of little help because they may not have physical similarity with the Nature or with the
178 comprehensive models they mimic. On the other hand, three-dimensional and intermediate-complexity
179 models do have, indeed, all the physics needed, but, as we have already discussed in the Introduction,
180 they may not be able to resolve the mass influx that may be responsible for a timescale of about few
181 hundreds of thousands years. Indeed, if a characteristic thickness of ice is a few thousands meters, then
182 we are talking about mass influx of the order of few centimeters per year. We nevertheless hope, that,
183 other than VCV18, simple but physics-based models can be designed to support (or reject) the
184 Milankovitch theory formulated here as an initial value problem.

185

186 **Competing interests:** The author has declared that there are no competing interests.



187

188 **References**

189

190 Abe-Ouchi, A., Saito, F., Kawamura, K., Raymo, M. E., Okuno, J. I., Takahashi, K., and Blatter, H.:
191 Insolation-driven 100,000-year glacial cycles and hysteresis of ice-sheet volume, *Nature*, 500, 190–194,
192 2013.

193

194 Bahr, D. B., Pfeffer, W. T., and Kaser, G.: A review of volume-area scaling of glaciers, *Rev. Geophys.*,
195 53,95–140, doi:10.1002/2014RG000470, 2015.

196

197 Ganopolski, A.: Toward generalized Milankovitch theory (GMT), *Clim. Past*, 20, 151–185,
198 <https://doi.org/10.5194/cp-20-151-2024>, 2024.

199

200 Ganopolski, A. and Calov, R.: The role of orbital forcing, carbon dioxide and regolith in 100 kyr glacial
201 cycles, *Clim. Past.*, 7, 1415–1425, <https://doi.org/10.5194/cp-7-1415-2011>, 2011.

202

203 Gowan, E.J.: Bayesian analysis and paleo ice sheet modelling: a commentary on the proposal by Tarasov
204 and Goldstein. [https://egusphere.copernicus.org/preprints/2023/egusphere-2022-1410/egusphere-2022-
205 1410-RC2-supplement.pdf](https://egusphere.copernicus.org/preprints/2023/egusphere-2022-1410/egusphere-2022-1410-RC2-supplement.pdf), 2023.

206

207 Saltzman, B.: Finite amplitude free convection as an initial value problem, *Journal of atmospheric
sciences*, 19, 4, 329-341, 1962.

208

209 Saltzman, B.: Dynamical paleoclimatology: generalized theory of global climate change, in: Vol. 80,
Academic Press, San Diego, CA, ISBN 0126173311, 2002.

210

211 Verbitsky, M.Y.: Equilibrium ice sheet scaling in climate modeling, *Climate Dynamics*, 7, 105–110,
<https://doi.org/10.1007/BF00209611>, 1992.

212

213 Verbitsky, M. Y.: Inarticulate past: similarity properties of the ice–climate system and their implications
214 for paleo-record attribution, *Earth Syst. Dynam.*, 13, 879–884, <https://doi.org/10.5194/esd-13-879-2022>,
2022.

215

216 Verbitsky, M. Y. and Crucifix, M.: π -theorem generalization of the ice-age theory, *Earth Syst. Dynam.*,
11, 281–289, <https://doi.org/10.5194/esd-11-281-2020>, 2020.

217

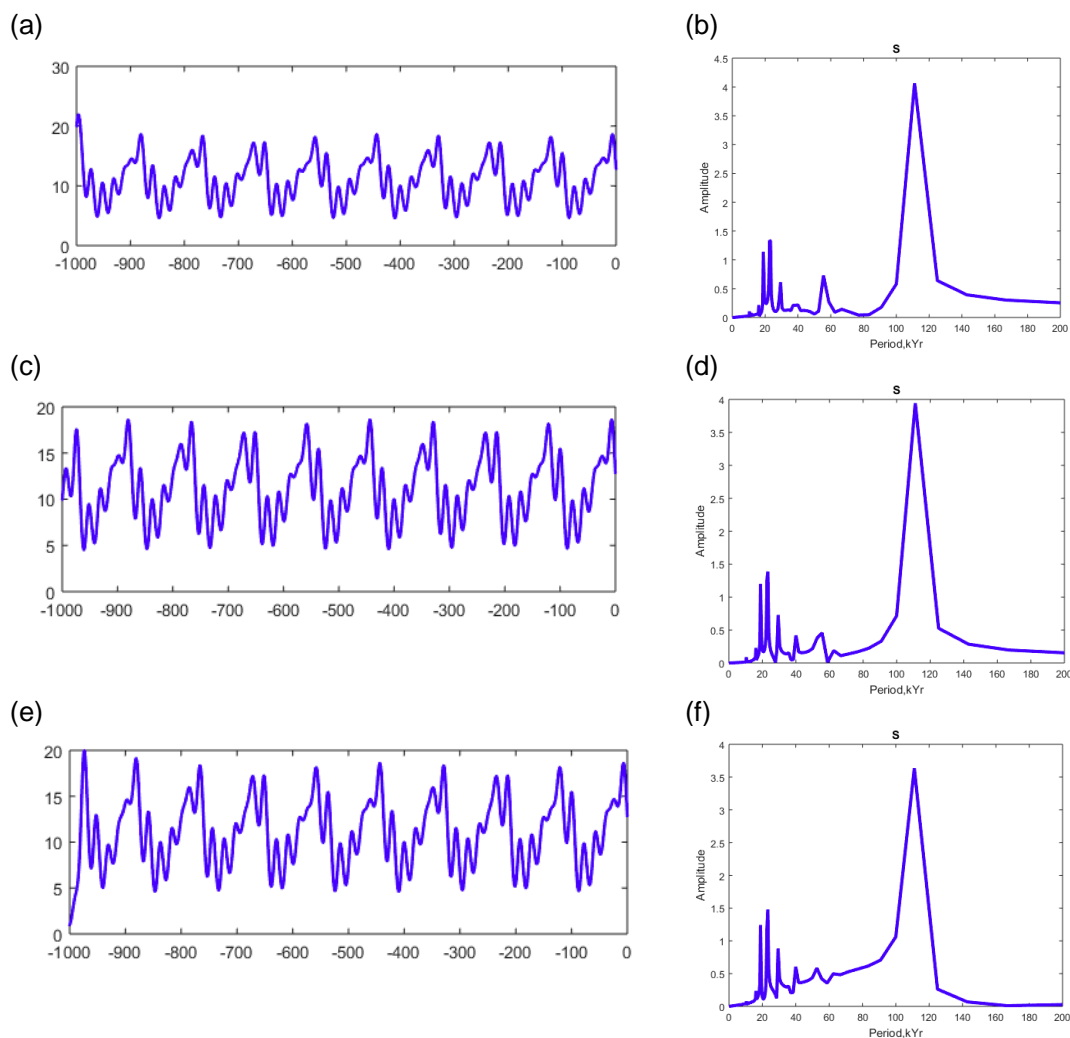
218 Verbitsky, M. Y. and Crucifix, M.: Do phenomenological dynamical paleoclimate models have physical
219 similarity with Nature? Seemingly, not all of them do, *Clim. Past*, 19, 1793–1803,
<https://doi.org/10.5194/cp-19-1793-2023>, 2023.

220

221 Verbitsky, M. Y., Crucifix, M., and Volobuev, D. M.: A theory of Pleistocene glacial rhythmicity, *Earth
Syst. Dynam.*, 9, 1025–1043, <https://doi.org/10.5194/esd-9-1025-2018>, 2018.



222



223

224

225

226

227

228

229

230

231

232

233

234

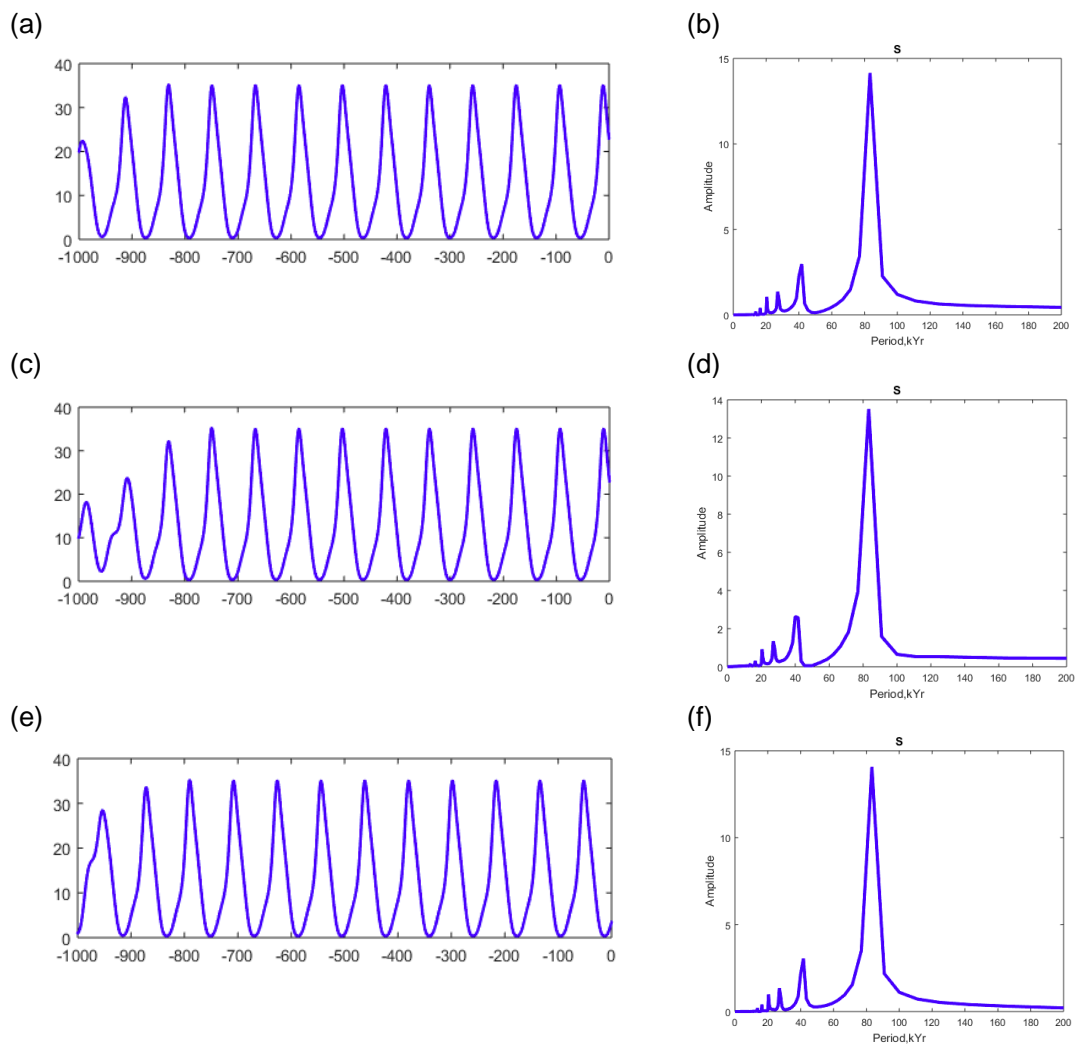
Figure 1. The dynamical system response to pure eccentricity-modulated precession, $F =$

$$\sin\left(\frac{2\pi t}{19}\right) + \sin\left(\frac{2\pi t}{23}\right).$$

(a), (c), and (e) are the time series of the area of glaciation in (10^6 km^2); **(b), (d), and (f)** are the corresponding spectral diagrams; **(a)** and **(b)** are for $S(0) = 20 \times 10^6 \text{ km}^2$; **(c)** and **(d)** are for $S(0) = 10 \times 10^6 \text{ km}^2$; **(e)** and **(f)** are for $S(0) = 1 \times 10^6 \text{ km}^2$.



235



236

237

Figure 2. The dynamical system response to pure obliquity forcing, $F = 1.0 \sin\left(\frac{2\pi t}{41}\right)$.

238

239

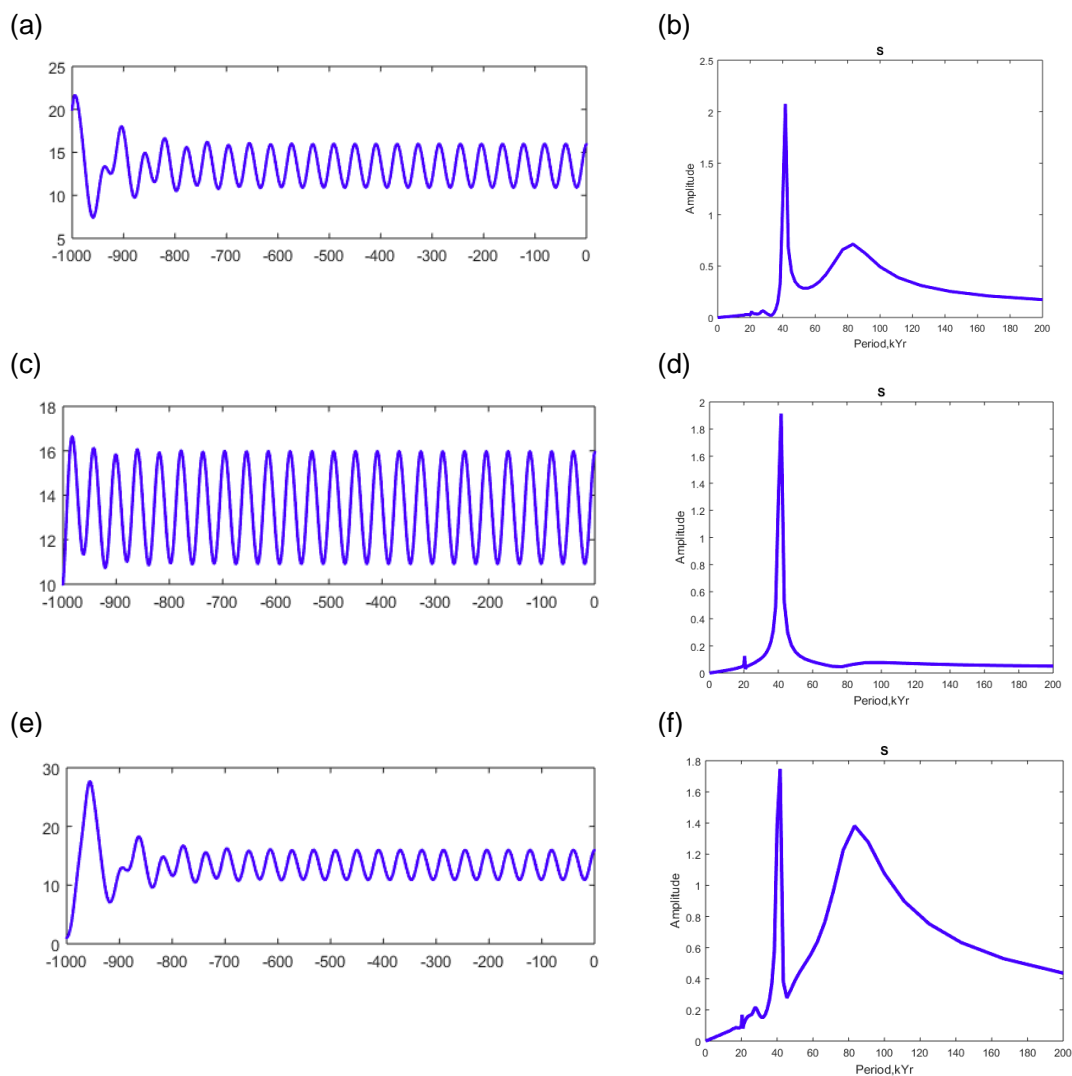
240

241

242

243

(a), (c), and (e) are the time series of the area of glaciation in (10^6 km^2); (b), (d), and (f) are the corresponding spectral diagrams; (a) and (b) are for $S(0) = 20 \cdot 10^6 \text{ km}^2$; (c) and (d) are for $S(0) = 10 \cdot 10^6 \text{ km}^2$; (e) and (f) are for $S(0) = 1 \cdot 10^6 \text{ km}^2$.



244

245

Figure 3. The dynamical system response to pure obliquity forcing, $F = 0.5 \sin\left(\frac{2\pi t}{41}\right)$.

246

247

(a), (c), and (e) are the time series of the area of glaciation in (10^6 km^2); (b), (d), and (f) are the

248

corresponding spectral diagrams; (a) and (b) are for $S(0) = 20 \cdot 10^6 \text{ km}^2$; (c) and (d) are for $S(0) = 10 \cdot 10^6$

249

km^2 ; (e) and (f) are for $S(0) = 1 \cdot 10^6 \text{ km}^2$.

250

251

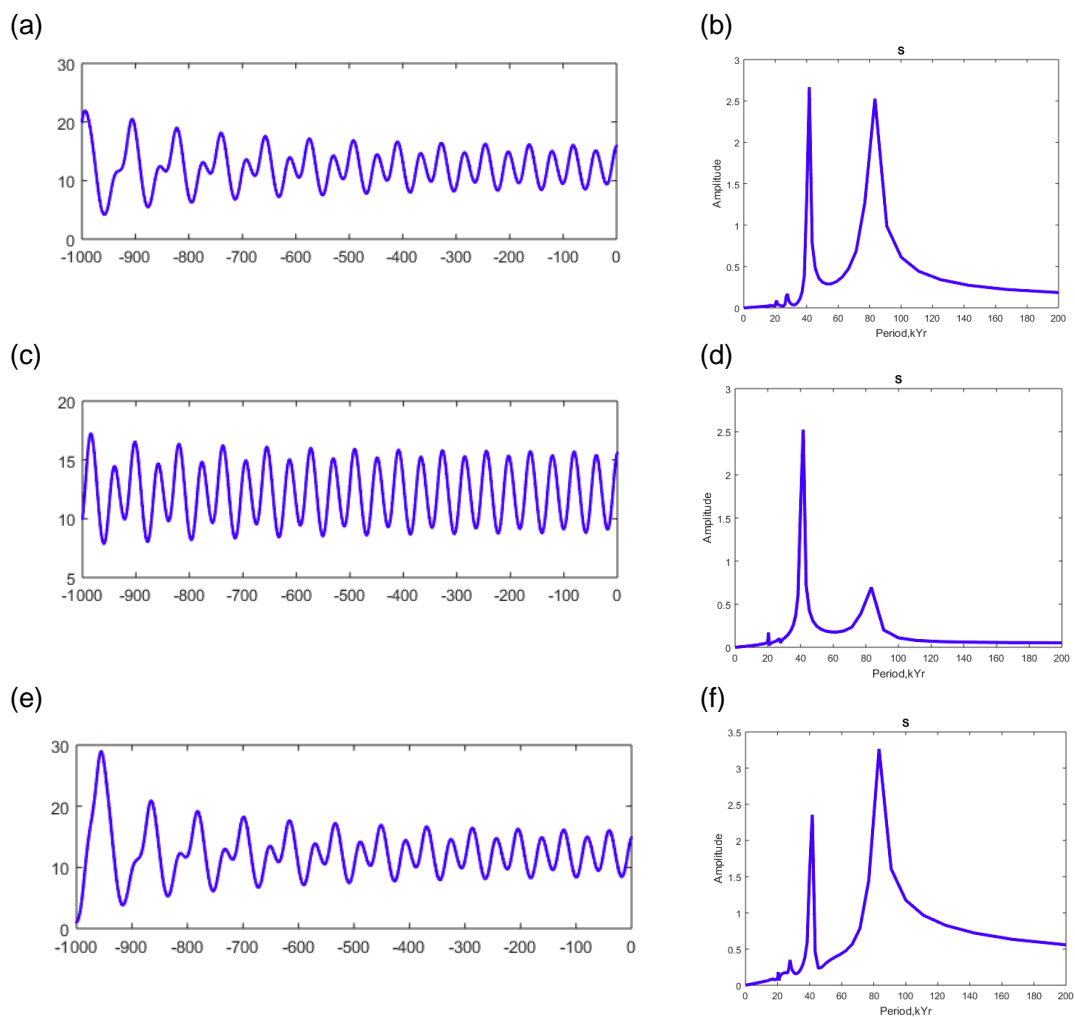
252

253

254

255

256



257

258

Figure 4. The dynamical system response to pure obliquity forcing, $F = 0.7 \sin\left(\frac{2\pi t}{41}\right)$.

259

260

(a), (c), and (e) are the time series of the area of glaciation in (10^6 km^2); (b), (d), and (f) are the

261

corresponding spectral diagrams; (a) and (b) are for $S(0) = 20 \cdot 10^6 \text{ km}^2$; (c) and (d) are for $S(0) = 10 \cdot 10^6$

262

km^2 ; (e) and (f) are for $S(0) = 1 \cdot 10^6 \text{ km}^2$.

263

264

265

266

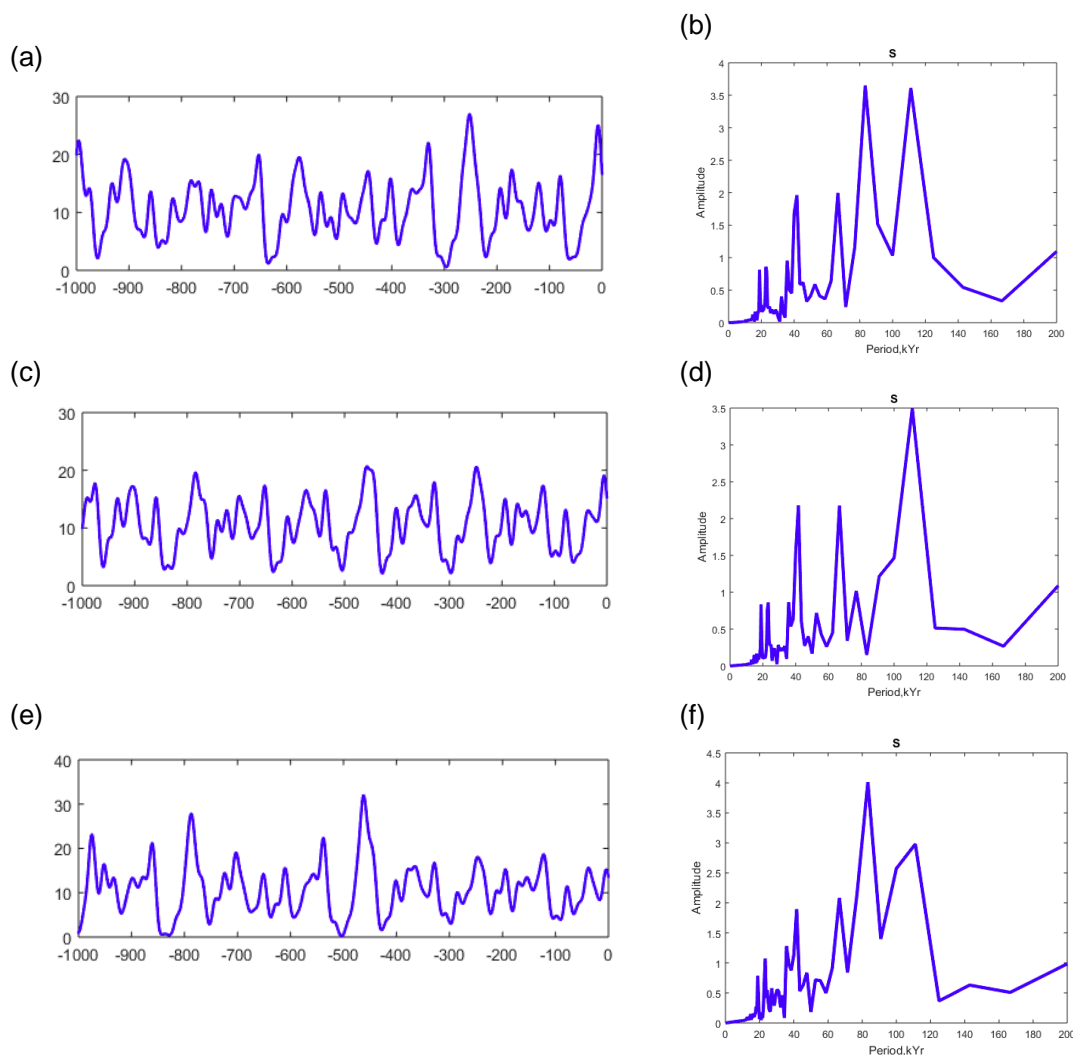
267

268

269

270

271



272

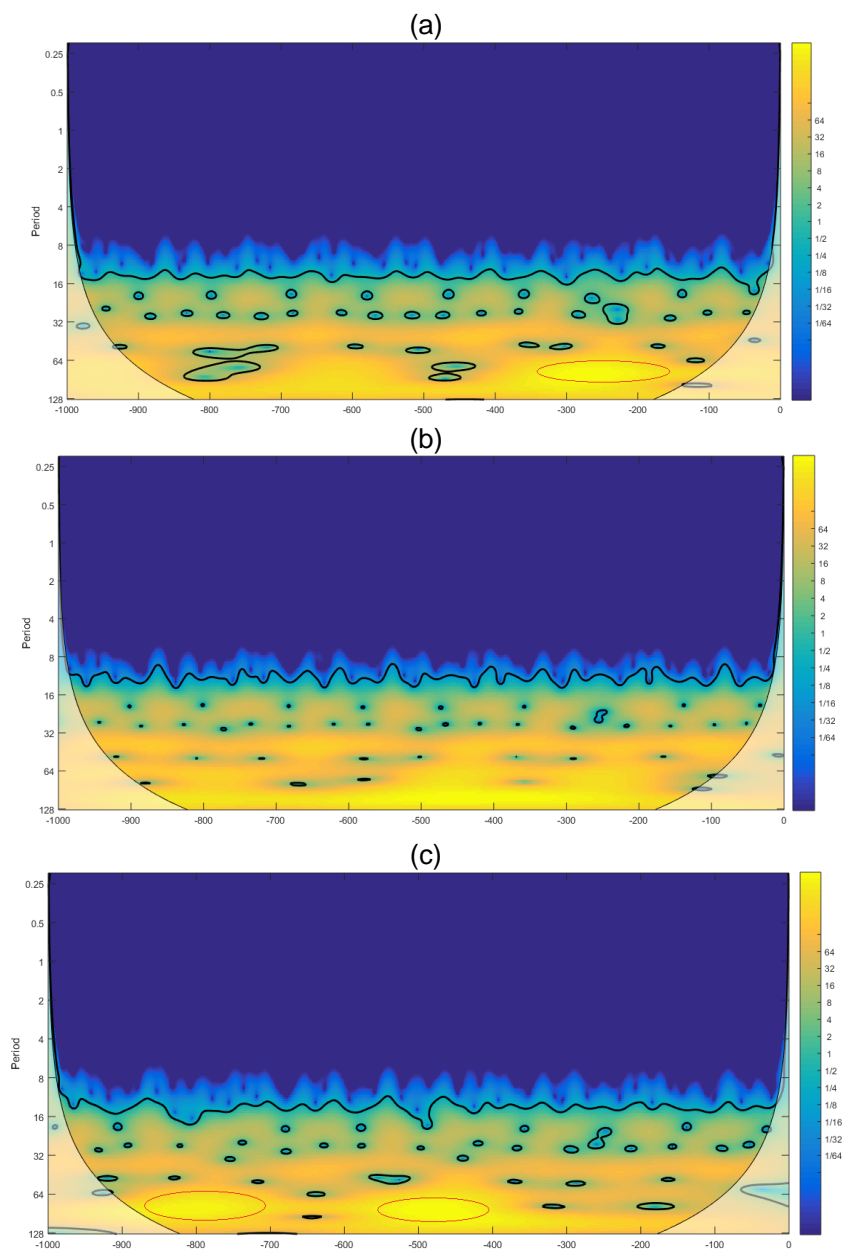
273 **Figure 5. The dynamical system response to orbital forcing, $F = 0.7 \left(\sin \left(\frac{2\pi t}{19} \right) + \sin \left(\frac{2\pi t}{23} \right) \right) +$**

274 **$0.7 \sin \left(\frac{2\pi t}{41} \right)$.**

275

276 **(a), (c), and (e) are the time series of the area of glaciation in (10^6 km²); (b), (d), and (f) are the**
 277 **corresponding spectral diagrams; (a) and (b) are for $S(0) = 20 \cdot 10^6$ km²; (c) and (d) are for $S(0) = 10 \cdot 10^6$**
 278 **km²; (e) and (f) are for $S(0) = 1 \cdot 10^6$ km².**

279



280

281 **Figure 6.** The dynamical system response to orbital forcing, $F = 0.7 \left(\sin\left(\frac{2\pi t}{19}\right) + \sin\left(\frac{2\pi t}{23}\right) \right) +$

282 $0.7 \sin\left(\frac{2\pi t}{41}\right)$.

283

284 The evolution of wavelet spectra for the time series of Fig. 5; (a) $S(0) = 20 \cdot 10^6 \text{ km}^2$; (b) $S(0) = 10$

285 10^6 km^2 ; (c) $S(0) = 1 \cdot 10^6 \text{ km}^2$. The red ellipses show the episodes of 80-kyr dominance.